

M^{III}Dy^{III}₃ (M = Fe^{III}, Co^{III}) Complexes: Three-Blade Propellers Exhibiting Slow Relaxation of Magnetization

Gong-Feng Xu,^{†,‡} Patrick Gamez,[§] Jinkui Tang,^{*,†} Rodolphe Clérac,^{*,||,⊥} Yun-Nan Guo,[†] and Yang Guo[†]

[†]State Key Laboratory of Rare Earth Resource Utilization, Changchun Institute of Applied Chemistry, Chinese Academy of Sciences, Changchun 130022, China

[‡]Department of Chemistry, College of Science, Tianjin University of Commerce, Tianjin 300134, China

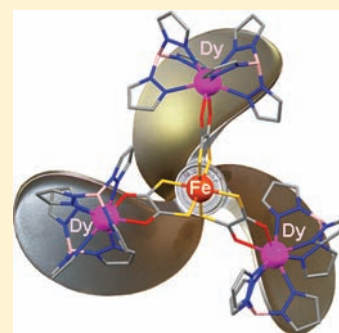
[§]Departament de Química Inorgànica, QBI, Universitat de Barcelona, Barcelona 08028, Spain

^{||}CNRS, CRPP, UPR 8641, F-33600 Pessac, France

[⊥]University of Bordeaux, CRPP, UPR 8641, F-33600 Pessac, France

S Supporting Information

ABSTRACT: [Dy^{III}(HBpz₃)₂]²⁺ moieties (HBpz₃⁻ = hydrotris(pyrazolyl)borate) and a 3d transition-metal ion (Fe^{III} or Co^{III}) have been rationally assembled using an dithiooxalato dianion ligand into 3d-4f [MDy₃(HBpz₃)₆(dto)₃]·4CH₃CN·2CH₂Cl₂ (M = Fe (1), Co (2)) complexes. Single-crystal X-ray studies reveal that three eight-coordinated Dy^{III} centers in a square antiprismatic coordination environment are connecting to a central octahedral trivalent Fe or Co ion forming a propeller-type complex. The dynamics of the magnetization in the two isostructural compounds, modulated by the nature of the central M^{III} metal ion, are remarkably different despite their analogous direct current (dc) magnetic properties. The slow relaxation of the magnetization observed for 2 mainly originates from isolated Dy ions, since a diamagnetic Co^{III} metal ion links the magnetic Dy^{III} ions. In the case of 1, the magnetic interaction between S = 1/2 Fe^{III} ion and the three Dy^{III} magnetic centers, although weak, generates a complex energy spectrum of magnetic states with low-lying excited states that induce a smaller energy gap than for 2 and thus a faster relaxation of the magnetization.



INTRODUCTION

Since the discovery of Single-Molecule Magnets (SMMs) in a dodecanuclear manganese complex,¹ intensive research efforts have been devoted in the quest for new SMMs.² These complexes behave as magnets at low temperatures, in other words, their field-induced magnetization relaxes slowly upon removal of the applied direct current (dc) field.³ Therefore, the fantastic interest of the scientific community for SMMs is motivated by their numerous potential applications, which include quantum computation,⁴ information storage,⁵ and biomedical purposes.⁶ Equally remarkable has been the magnetic refrigeration brought about by the molecules similar to the SMMs, albeit with small magnetic anisotropy.⁷

Historically, the field of SMMs has grown tremendously through the design and preparation of systems containing 3d metal ions.^{2a} Recently, the development of mononuclear lanthanide complexes with long magnetization relaxation times has initiated extensive research investigations on 4f-based SMMs.⁸ In addition, the use of different spin carriers (such as 3d-4f) represents a very active synthetic approach for designing low-dimensional molecular magnets, as it allows to combine a high-spin ground state with a large uniaxial magnetic anisotropy.⁹ Thus, a few 3d-4f complexes with diverse topologies exhibiting SMM behavior have been reported.^{9a,10} Recently, we have shown that the oxalate dianion (ox²⁻) can bridge efficiently two capped Dy^{III} building units (the capping

ligand being hydrotris(pyrazolyl)borate; HBpz₃⁻), generating intramolecular ferromagnetic interactions.¹¹ In the present work, we report on a rational synthetic strategy to connect 4f [Dy(HBpz₃)₂]²⁺ moieties to a 3d transition-metal ion (Fe^{III} or Co^{III}), using an oxalato-type anionic ligand leading to heterometallic M^{III}Dy^{III}₃ complexes exhibiting slow relaxation of their magnetization.

Inspired by the previously reported [Dy₂(HBpz₃)₄(μ-ox)]·2CH₃CN·CH₂Cl₂ compound,¹¹ our initial approach has been to react aqueous solutions of DyCl₃·6H₂O/K(HBpz₃) and Fe^{III} (or Co^{III}) salt/K₂ox. Unfortunately, this synthetic approach produces instantly an unknown precipitate that was not possible to characterize. Subsequently, an alternative synthetic route for the preparation of the targeted discrete M^{III}/Dy^{III} complexes (M = Fe or Co) has been undertaken. It consists of the reaction of M(ox)₃ (M = Fe or Co) with an aqueous solution of DyCl₃·6H₂O and K(HBpz₃). Again, an unidentified solid is obtained as a product of this reaction. To synthesize finally M^{III}Dy^{III}₃ complexes, we decided to use the bridging dithiooxalato dianion (dto²⁻) with the idea that the “soft” sulfur atoms of the asymmetric dto²⁻ ligand will preferably coordinate the “soft” metal ions in contrast to the “hard” oxygen atoms that should rather bind to “hard” metal

Received: January 18, 2012

Published: May 7, 2012

Table 1. Crystal Data and Structure Refinement for [FeDy₃(HBpz₃)₆(dto)₃]·4CH₃CN·2CH₂Cl₂ (1) and [CoDy₃(HBpz₃)₆(dto)₃]·4CH₃CN·2CH₂Cl₂ (2)

	1	2
empirical formula	C ₇₀ H ₇₆ B ₆ Cl ₄ Dy ₃ FeN ₄₀ O ₆ S ₆	C ₇₀ H ₇₆ B ₆ Cl ₄ Dy ₃ CoN ₄₀ O ₆ S ₆
F _w (g mol ⁻¹)	2516.08	2519.16
crystal system	monoclinic	monoclinic
space group	C2/c	C2/c
crystal color	dark blue-violet	red
crystal size (mm ³)	0.23 × 0.25 × 0.26	0.20 × 0.18 × 0.16
temperature (K)	153(2)	166(2)
a (Å)	28.255(5)	28.3220(13)
b (Å)	24.796(5)	24.7043(12)
c (Å)	18.738(5)	18.6907(9)
β (deg)	131.050(5)	131.1310(10)
V (Å ³)	9900(4)	9850.0(8)
ρ _{calcd} (Mg/m ³)	1.677	1.699
μ (mm ⁻¹)	2.685	2.720
F(000)	4904	4972
θ for data collection (deg)	1.91–25.00	2.18–25.00
collected reflections	29965	26080
independent reflections	7458	6668
R _{int}	0.0298	0.0449
R [I > 2σ(I)]	0.0398	0.0434
wR (all data)	0.1119	0.1195
goodness of fit on F ²	1.094	1.029
largest diff. peak and hole (e Å ⁻³)	−2.179 and 2.331	−1.879 and 1.774

ions.¹² Earlier studies on the dithiooxalate ligand revealed its unique coordination properties.¹³ According to the hard-soft acid-base (HSAB) theory, rare-earth ions like Dy^{III} are hard acids,¹⁴ and thus are expected to coordinate to dto²⁻ anions through their oxygen atoms. On the other hand, soft 3d metal ions like Fe^{III} or Co^{III} should bind to the sulfur atoms. Therefore, the use of this particular asymmetric ligand is crucial to allow good control of the final heterometallic coordination compound. Propeller-like M^{III}Dy^{III}₃ (M = Fe, Co) compounds have been successfully assembled by applying this rational synthetic strategy. Single-crystal X-ray studies reveal that both compounds are isostructural, thus providing a unique opportunity to experimentally probe the differences in the magnetic properties on replacing the S = 1/2 Fe^{III} ion with the S = 0 Co^{III} ion. Detailed magnetization dynamics studies show that these unique three-bladed propellers exhibit slow relaxation of their magnetization modulated by the nature of the central M^{III} metal ion.

EXPERIMENTAL SECTION

General Procedures. All chemicals were used as commercially obtained without further purification. Elemental analysis for C, H, and N were carried out on a Perkin-Elmer 2400 analyzer. FTIR spectra were recorded with a Perkin-Elmer Fourier transform infrared spectrophotometer using the reflectance technique (4000–300 cm⁻¹). Samples were prepared as KBr disks. The magnetic susceptibility measurements were obtained with the use of a MPMS-XL Quantum Design SQUID magnetometer and a PPMS-9 susceptometer housed at the Centre de Recherche Paul Pascal. The magnetometer and the susceptometer work between 1.8 and 400 K for dc applied fields ranging from −7 to 7 T (MPMS-XL). Alternating current (ac) susceptibility measurements were made with an oscillating ac field of 1 Oe with frequency between 10 to 10000 Hz (PPMS-9). Measurements were performed on polycrystalline samples (10.36 and 11.17 mg for 1 and 2), introduced in a sealed polyethylene bag (3 × 0.5 × 0.02 cm). The magnetic data were corrected for the sample holder and the diamagnetic contributions.

X-ray Crystallography. Crystallographic data and refinement details are given in Table 1. Suitable single crystals with dimensions of 0.23 × 0.25 × 0.26 mm³ and 0.20 × 0.18 × 0.16 mm³ for 1 and 2, respectively, were selected for single-crystal X-ray diffraction analysis. Crystallographic data were collected at 153(2) K (1) and 166(2) K (2) on a Bruker ApexII CCD diffractometer with graphite monochromated Mo Kα radiation (λ = 0.71073 Å). Data processing was accomplished with the SAINT processing program.¹⁵ The structure was solved by the direct methods and refined on F² by full-matrix least-squares using SHELXL97.¹⁶ CCDC-831217 (1) and 831218 (2) contain the supplementary crystallographic data for this paper. These data can be obtained free of charge from the Cambridge Crystallographic Data Centre via www.ccdc.cam.ac.uk/data_request/cif.

Synthesis of 1. An aqueous solution (10 mL) of DyCl₃·6H₂O (0.3 mmol, 0.1131 g) and an aqueous solution (10 mL) of K(HBpz₃)¹⁷ (0.6 mmol, 0.1513 g) were added simultaneously to a stirred aqueous solution (20 mL) containing FeCl₃·6H₂O (0.1 mmol, 0.0270 g) and Na₂dto¹⁸ (0.3 mmol, 0.0498 g). The solution was stirred for 5 min, and then cooled in a refrigerator overnight. The resulting pale-blue precipitate was filtered off, washed three times with water, and dried under vacuum. The crude product was recrystallized from dichloromethane-acetonitrile, and suitable single crystals for X-ray diffraction analysis were obtained in the dark (yield = 12%). IR (KBr, cm⁻¹): ν = 2492, 1494, 1402, 1310, 1211, 1110, 1042, 760, 718, 620. Anal. Calcd for C₇₀H₇₆B₆Cl₄Dy₃FeN₄₀O₆S₆: C, 33.42; H, 3.04; N, 22.27. Found: C, 33.65; H, 2.86; N, 21.93.

Synthesis of 2. This compound was prepared applying a similar procedure with an aqueous solution of [Co(NH₃)₆]Cl₃¹⁹ (0.1 mmol, 0.0267 g) and Na₂dto (0.3 mmol, 0.0498 g) heated to 80 °C for several minutes, and subsequently cooled to room temperature. The red crude product was recrystallized from dichloromethane-acetonitrile and suitable single crystals for X-ray diffraction analysis were obtained (yield = 65%). IR (KBr, cm⁻¹): ν = 2462, 1505, 1405, 1301, 1215, 1122, 1050, 761, 722, 620. Anal. Calcd for C₇₀H₇₆B₆Cl₄Dy₃CoN₄₀O₆S₆: C, 33.38; H, 3.04; N, 22.24. Found: C, 33.56; H, 2.90; N, 22.45.

RESULTS AND DISCUSSION

Crystal Structures. The reaction of aqueous solutions of $\text{DyCl}_3 \cdot 6\text{H}_2\text{O}/\text{K}(\text{HBpz}_3)$ and $\text{FeCl}_3 \cdot 6\text{H}_2\text{O}$ or $[\text{Co}(\text{NH}_3)_6]\text{Cl}_3/\text{Na}_2\text{dto}$ yields the desired heterotetranuclear compounds $[\text{FeDy}_3(\text{HBpz}_3)_6(\text{dto})_3] \cdot 4\text{CH}_3\text{CN} \cdot 2\text{CH}_2\text{Cl}_2$ (**1**) with 12% yield or $[\text{CoDy}_3(\text{HBpz}_3)_6(\text{dto})_3] \cdot 4\text{CH}_3\text{CN} \cdot 2\text{CH}_2\text{Cl}_2$ (**2**) with 65% yield.

Single-crystal X-ray studies (see Supporting Information) reveal that **1** and **2** are isostructural and crystallize in the monoclinic $C2/c$ space group. Perspective views of the molecular structure of **1** and **2** are shown in Figure 1 and

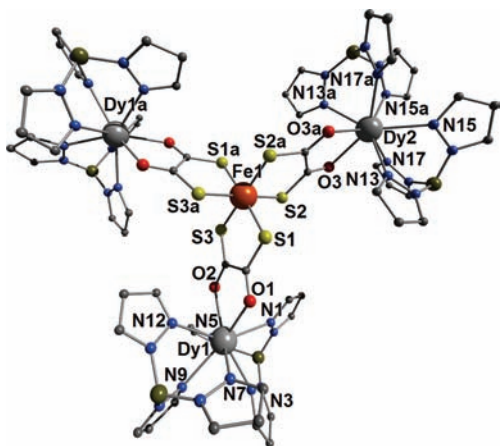


Figure 1. Representation of compound **1** with the atom-numbering scheme. Hydrogen atoms and lattice solvent molecules are not shown for clarity. Symmetry operation: $a = 2 - x, y, 1/2 - z$.

Supporting Information, Figure S1, respectively. Details about the structure solution and refinement are summarized in Table 1, and selected bond distances and angles are listed in Supporting Information, Tables S1 and S2. In these compounds, the tetranuclear $\text{M}^{\text{III}}\text{Dy}^{\text{III}}_3$ complexes adopt a propeller-type geometry consisting of three eight-coordinated Dy^{III} centers in a square antiprismatic coordination environment, which are connected to a central octahedral trivalent Fe or Co ion (Figure 1–2 and Supporting Information, Figure S1).

The two square bases of the Dy1 antiprism coordination sphere are formed by the (O1, N1, N3, and N7) and (O2, N5, N9, and N12) set of atoms (Figure 2A). As anticipated, the

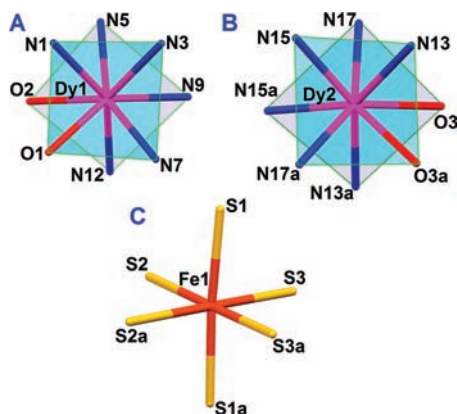


Figure 2. Coordination environment of the dysprosium(III) ions: Dy1 (A), Dy2 (B), and of the iron(III) Fe1 (C). Symmetry operation: $a = 2 - x, y, 1/2 - z$.

Dy1 ion is coordinated by six nitrogen atoms belonging to two HBpz_3^- ligands, and two oxygen atoms from a dto^{2-} anion. The Dy–N and Dy–O bond distances as well as the Dy^{III} coordination geometry are comparable to those observed for $[\text{Dy}_2(\text{HBpz}_3)_4(\mu\text{-ox})] \cdot 2\text{CH}_3\text{CN} \cdot \text{CH}_2\text{Cl}_2$.¹¹ Dy2 exhibits a similar environment with slight variations of the metric parameters (Supporting Information, Table S1 and Figure 2B). Each Dy ion is connected to a Fe center, via a bridging dto^{2-} . Hence, Fe1 is in an octahedral environment formed by six sulfur atoms belonging to three different dithiooxalato ligands (Figure 2C). The Fe–S bond lengths and angles (Supporting Information, Table S1) are typical of FeS_6 octahedral coordination spheres.²⁰

The crystal lattice contains the two enantiomeric isomers of **1** with the central iron(III) atom Fe1 adopting two enantiomeric conformations, namely, the Λ and Δ isomers (Figure 3A).

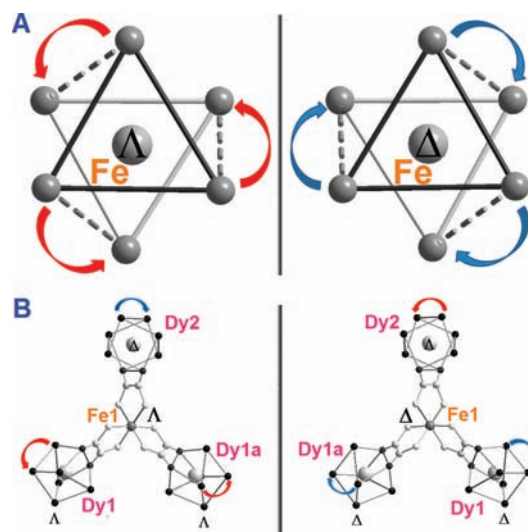


Figure 3. Illustrations of the two coordination enantiomers present in the crystal lattice of **1**. (A) Λ and Δ forms of the central Fe atom; (B) $\Lambda/\Lambda, \Lambda, \Delta$ and $\Delta/\Delta, \Delta, \Lambda$ isomers of the $\text{Fe}^{\text{III}}\text{Dy}^{\text{III}}_3$ core.

Interestingly, the Dy1 (Dy1a) and Dy2 atoms exhibit opposite configurations, generating a Λ, Λ, Δ propeller for the Λ Fe1 center, and a Δ, Δ, Λ one for the other enantiomer (Figure 3B). Thus, in contrast with the other 3d-4f propellers reported in the literature,²¹ the present $\text{Fe}^{\text{III}}\text{Dy}^{\text{III}}_3$ system does not possess a C_3 -symmetry, the Dy^{III} ions Dy1 (or Dy1a) and Dy2 being nonequivalent. The same peculiar structural characteristics are noticed for **2**.

The replacement of iron(III) by cobalt(III) leads to the isostructural compound $[\text{Dy}_3\text{Co}(\text{HBpz}_3)_6(\text{dto})_3] \cdot 4\text{CH}_3\text{CN} \cdot 2\text{CH}_2\text{Cl}_2$ (**2**). Its single-crystal X-ray structure is depicted in Supporting Information, Figure S1. The bond lengths and angles are very close to those observed for **1** (Supporting Information, Tables S1 and S2). In particular, the Dy–Dy separation distances and the Dy–M–Dy angles are almost identical (Supporting Information, Tables S1 and S2, Figure S2), which is an important feature regarding the magnetic-exchange coupling between the 3d and 4f ions as well as the contribution of central metal ion to the relaxation dynamics of these propeller-like compounds (vide infra).

Magnetic Properties. Direct-current (dc) magnetic susceptibility studies of **1** and **2** have been carried out in an

applied magnetic field of 1 kOe in the 300–1.8 K temperature range. The χT versus T data, where χ is the molar magnetic susceptibility, are shown in Figure 4. The observed χT value at

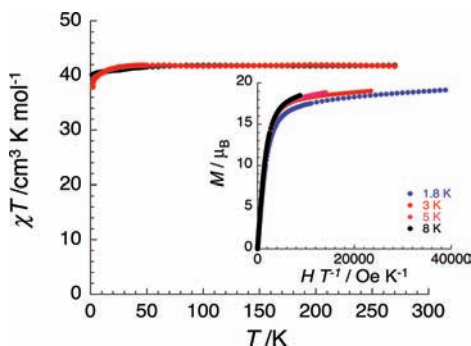


Figure 4. Temperature dependence of χT product (χ being the magnetic susceptibility defined as M/H per $M^{\text{III}}\text{Dy}^{\text{III}}_3$ complex) at 1 kOe for **1** (black) and **2** (red). Inset: M versus H/T plot at different temperatures below 8 K for **1**.

300 K of 41.8 and 41.7 $\text{cm}^3 \text{K mol}^{-1}$ for **1** and **2** are close to the expected values (42.875 and 42.50 $\text{cm}^3 \text{K mol}^{-1}$, respectively) for three uncoupled Dy^{III} ions ($S = 5/2$, $L = 5$, ${}^6\text{H}_{15/2}$, $g = 4/3$) and one low-spin $S = 1/2$ Fe^{III} ion or one diamagnetic Co^{III} ion. The χT product remains roughly constant until 50 K and then decreases to reach a minimum of 40.1 and 37.9 $\text{cm}^3 \text{K mol}^{-1}$ for **1** and **2** at 1.8 K, indicating very weak intramolecular magnetic interaction between spin carriers. The nonsuperimposition of the M versus H/T data on a single master-curve (Figure 4 and Supporting Information, Figures S3–S4) suggests the presence of a significant magnetic anisotropy, likely coming from the Dy^{III} metal ions, and/or low-lying excited states, in agreement with weak intramolecular magnetic interactions, in both **1** and **2**.¹¹ As expected, the dc magnetic properties of **1** and **2** look almost the same; however, the dynamics of the magnetization in the two compounds is dramatically different (vide infra).

Both the temperature and frequency dependences of the ac susceptibilities for **1** and **2** have been measured under zero-dc field (Figure 5 and Supporting Information, Figures S5–S8). A frequency dependence of the ac susceptibilities is observed for both compounds with an out-of-phase component that is weak in intensity and that does not display a maximum in the experimental temperature (above 1.8 K) and frequencies (1 to 10000 Hz) windows. This result suggests the presence of a fast relaxation of the magnetization (below 10^{-5} s) as expected in the presence of zero-field quantum tunnelling of the magnetization (QTM) often observed for low symmetry lanthanide based-SMMs.^{8a,22} To check for the presence of QTM, ac measurements were performed under small dc fields ($H \leq 1500$ Oe) that are expected to lift the degeneracy of the $\pm m_s$ levels, decrease the probability of QTM, and hence increase the relaxation time, τ .^{22b} Indeed, the application of a dc field causes a drastic reduction of the characteristic frequency from above 10000 Hz (at $H = 0$ Oe) to a minimum value of 4800 and 3.3 Hz for **1** and **2** respectively, at same optimum field of about 800 Oe (Supporting Information, Figures S9–S11). As suspected, these results highlight the presence of significantly fast QTM in zero-dc field. At the optimum field of 800 Oe for which the QTM probability is minimized, the ac susceptibility has been measured for both complexes (Figure 6 and Supporting Information, Figures S12–15).

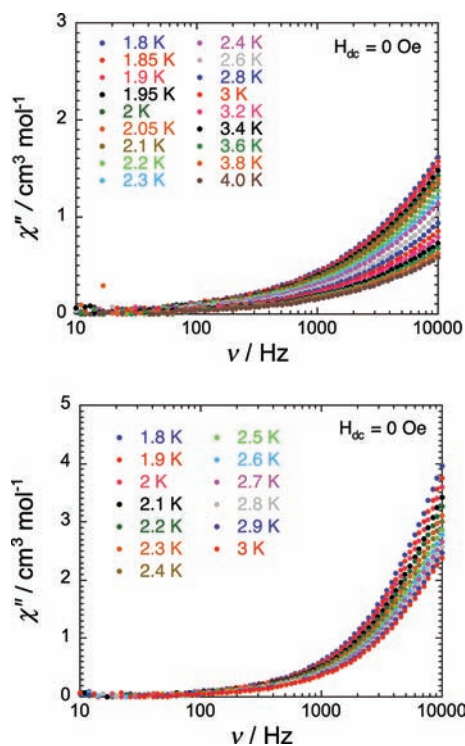


Figure 5. Frequency dependence of the out-of-phase ac susceptibility (χ'') of **1** (top) and **2** (bottom), under zero-dc field.

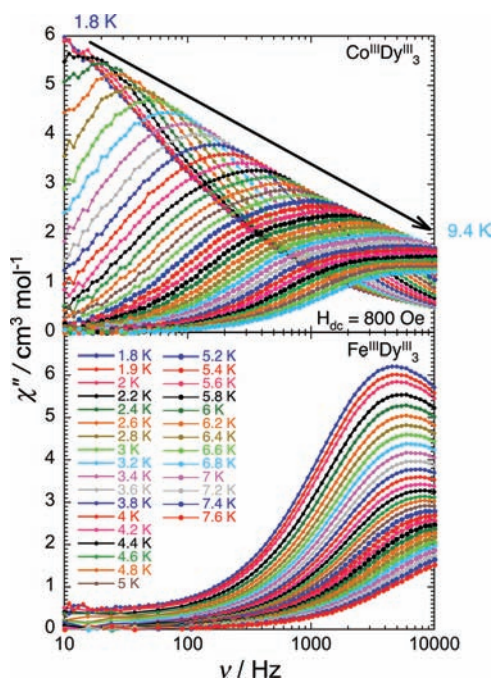


Figure 6. Frequency dependence of the out-of-phase ac susceptibility (χ'') of **1** (bottom) and **2** (top), under 800 Oe dc field.

For both compounds, the ac susceptibility at 800 Oe possesses a frequency dependent out-of-phase component that exhibits a clear maximum above 1.8 K (Figure 6). Hence, the temperature dependence of the relaxation time can be deduced as shown in Figure 7 and Supporting Information, Figures S16–S17. When τ is plotted in a semilogarithmic scale as a function of T^{-1} (Figure 7), it is clear that the temperature dependence of the relaxation is not a simple Arrhenius law, that

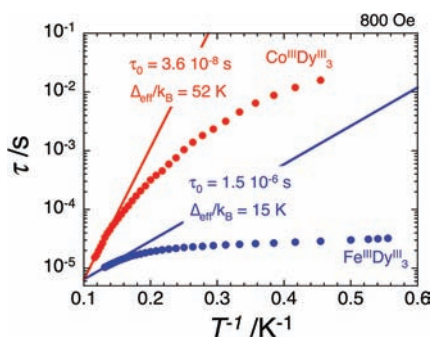


Figure 7. Magnetization relaxation time, τ , versus T^{-1} semilogarithmic plots for **1** (blue) and **2** (red) under 800 Oe dc field. The solid lines are the Arrhenius law obtained considering data at the highest temperatures (see text).

is, τ is not exponentially enhanced when the temperature decreases. Indeed, even under 800 Oe, the quantum pathway of magnetization relaxation is still operative with relaxation times smaller than 10^{-1} s, explaining the absence of M versus H hysteresis at the sweeping rate used in a classical magnetometer. Therefore it is difficult to evaluate the energy gap, Δ , associated with the thermally activated regime of relaxation. Nevertheless, a lower limit of the relaxation time can be estimated considering only the 6 highest temperatures for which the relaxation time can be estimated. The linear fit of the experimental data leads to a minimum energy gap, Δ_{\min} , and a preexponential factor, τ_0 , of 15 K and 1.5×10^{-6} s for **1** and 52 K and 3.6×10^{-8} s for **2**. It should be noticed that τ_0 , the attempt time of relaxation from the thermal bath, values are notably large in comparison to the expected values around 10^{-9} – 10^{-11} s for SMMs.^{2a,3b} These values are obviously enhanced by the presence of QTM even at 800 Oe confirming that the obtained Δ_{\min} must be taken as a lower limit of the real thermal energy gaps (Δ).

As shown above, the dynamics of the magnetization in the two isostructural compounds are remarkably different despite their analogous dc magnetic properties. The replacement of the diamagnetic Co^{III} ion by a paramagnetic Fe^{III} has thus a major impact on the relaxation time of these systems. In the case of **2**, the presence of a diamagnetic metal ion, Co^{III} , between the magnetic Dy^{III} ions is certainly leading to tiny inter-Dy magnetic interactions. Therefore, the slow relaxation observed for **2** is mainly originating from isolated Dy ions. It is worth noting that the Figure 6 is clearly showing a broad relaxation mode that certainly hides more than one relaxation process in agreement with the presence of two different Dy^{III} sites. In the case of **1**, the $S = 1/2$ Fe^{III} ion is interacting, probably weakly, with the three Dy^{III} magnetic centers. Therefore a complex energy spectrum of magnetic states is generated with low-lying excited states that induce a smaller energy gap than for **2** and thus a faster relaxation of the magnetization.

CONCLUSION

In summary, a synthetic strategy, taking advantage of the HSAB theory (Pearson acid base concept), has been applied successfully to design and prepare 3d-4f based coordination complexes with unusual magnetic properties. Propeller-like $\text{M}^{\text{III}}\text{Dy}^{\text{III}}_3$ ($\text{M} = \text{Fe}, \text{Co}$) compounds have been obtained, with Dy^{III} ions forming the blades of the propellers that adopt reverse enantiomeric configurations. These unique three-bladed

propellers exhibit slow relaxation of their magnetization modulated by the nature of the central M^{III} metal ion.

ASSOCIATED CONTENT

Supporting Information

Crystal data, additional crystallographic diagrams and magnetic diagrams. This material is available free of charge via the Internet at <http://pubs.acs.org>.

AUTHOR INFORMATION

Corresponding Author

*E-mail: tang@ciac.jl.cn (J.T.), clerac@crpp-bordeaux.cnrs.fr (R.C.).

Notes

The authors declare no competing financial interest.

ACKNOWLEDGMENTS

The authors thanks the National Natural Science Foundation of China (91022009 and 20921002), the Conseil Régional d'Aquitaine, GIS Advanced Materials in Aquitaine (COMET Project), the Université of Bordeaux, the CNRS and the ANR (NT09_469563, AC-MAGnets) for financial support.

REFERENCES

- (a) Sessoli, R.; Tsai, H. L.; Schake, A. R.; Wang, S.; Vincent, J. B.; Foltling, K.; Gatteschi, D.; Christou, G.; Hendrickson, D. N. *J. Am. Chem. Soc.* **1993**, *115*, 1804–1816. (b) Sessoli, R.; Gatteschi, D.; Caneschi, A.; Novak, M. A. *Nature* **1993**, *365*, 141–143.
- (a) Aromi, G.; Brechin, E. K. Synthesis of 3d Metallic Single-Molecule Magnets. In *Single-Molecule Magnets and Related Phenomena*; Winpenny, R., Ed.; Springer: Berlin, Germany, 2006; Vol. 122, p 1. (b) Murrie, M. *Chem. Soc. Rev.* **2010**, *39*, 1986–1995. (c) Kostakis, G. E.; Ako, A. M.; Powell, A. K. *Chem. Soc. Rev.* **2010**, *39*, 2238–2271. (d) Bagai, R.; Christou, G. *Chem. Soc. Rev.* **2009**, *38*, 1011–1026. (e) Tasiopoulos, A. J.; Perlepes, S. P. *Dalton Trans.* **2008**, 5537–5555.
- (a) Wernsdorfer, W.; Aliaga-Alcalde, N.; Hendrickson, D. N.; Christou, G. *Nature* **2002**, *416*, 406–409. (b) Gatteschi, D.; Sessoli, R. *Angew. Chem., Int. Ed.* **2003**, *42*, 268–297.
- (a) Leuenberger, M. N.; Loss, D. *Nature* **2001**, *410*, 789–793. (b) Cerletti, V.; Coish, W. A.; Gywat, O.; Loss, D. *Nanotechnology* **2005**, *16*, R27–R49. (c) Timco, G. A.; Faust, T. B.; Tuna, F.; Winpenny, R. E. P. *Chem. Soc. Rev.* **2011**, *40*, 3067–3075. (d) Aromi, G.; Aguilera, D.; Gamez, P.; Luis, F.; Roubeau, O. *Chem. Soc. Rev.* **2012**, 537–546.
- Bogani, L.; Wernsdorfer, W. *Nat. Mater.* **2008**, *7*, 179–186.
- Cage, B.; Russek, S. E.; Shoemaker, R.; Barker, A. J.; Stoldt, C.; Ramachandran, V.; Dalal, N. S. *Polyhedron* **2007**, *26*, 2413–2419.
- (a) Manoli, M.; Collins, A.; Parsons, S.; Candini, A.; Evangelisti, M.; Brechin, E. K. *J. Am. Chem. Soc.* **2008**, *130*, 11129–11139. (b) Evangelisti, M.; Brechin, E. K. *Dalton Trans.* **2010**, 4672–4676. (c) Evangelisti, M.; Roubeau, O.; Palacios, E.; Camón, A.; Hooper, T. N.; Brechin, E. K.; Alonso, J. J. *Angew. Chem., Int. Ed.* **2011**, *50*, 6606–6609. (d) Langley, S. K.; Chilton, N. F.; Moubaraki, B.; Hooper, T.; Brechin, E. K.; Evangelisti, M.; Murray, K. S. *Chem. Sci.* **2011**, *2*, 1166–1169. (e) Zheng, Y.-Z.; Evangelisti, M.; Winpenny, R. E. P. *Chem. Sci.* **2011**, *2*, 99–102. (f) Sessoli, R. *Angew. Chem., Int. Ed.* **2012**, *51*, 43–45.
- (a) Ishikawa, N.; Sugita, M.; Ishikawa, T.; Koshihara, S.-y.; Kaizu, Y. *J. Phys. Chem. B* **2004**, *108*, 11265–11271. (b) Rinehart, J. D.; Long, J. R. *Chem. Sci.* **2011**, *2*, 2078–2085.
- (a) Sessoli, R.; Powell, A. K. *Coord. Chem. Rev.* **2009**, *253*, 2328–2341. (b) Coulon, C.; Miyasaka, H.; Clérac, R. Single-Chain Magnets: Theoretical Approach and Experimental Systems. In *Single-Molecule Magnets and Related Phenomena*; Winpenny, R., Ed.; Springer: Berlin, Germany, 2006; Vol. 122, pp 163–206.

- (10) (a) Mori, F.; Nyui, T.; Ishida, T.; Nogami, T.; Choi, K. Y.; Nojiri, H. *J. Am. Chem. Soc.* **2006**, *128*, 1440–1441. (b) Aronica, C.; Pilet, G.; Chastanet, G.; Wernsdorfer, W.; Jacquot, J. F.; Luneau, D. *Angew. Chem., Int. Ed.* **2006**, *45*, 4659–4662. (c) Mereacre, V. M.; Ako, A. M.; Clérac, R.; Wernsdorfer, W.; Filoti, G.; Bartolome, J.; Anson, C. E.; Powell, A. K. *J. Am. Chem. Soc.* **2007**, *129*, 9248–9249. (d) Stamatatos, T. C.; Teat, S. J.; Wernsdorfer, W.; Christou, G. *Angew. Chem., Int. Ed.* **2009**, *48*, 521–524.
- (11) Xu, G.-F.; Wang, Q.-L.; Gamez, P.; Ma, Y.; Clérac, R.; Tang, J.; Yan, S.-P.; Cheng, P.; Liao, D.-Z. *Chem. Commun.* **2010**, *46*, 1506–1508.
- (12) Dietzsch, W.; Strauch, P.; Hoyer, E. *Coord. Chem. Rev.* **1992**, *121*, 43–130.
- (13) (a) Cox, E. G.; Wardlaw, W.; Webster, K. C. *J. Chem. Soc.* **1935**, 1475–1480. (b) Coucouvanis, D. *J. Am. Chem. Soc.* **1970**, *92*, 707–709.
- (14) Pearson, R. G. *J. Am. Chem. Soc.* **1963**, *85*, 3533–3539.
- (15) SAINT, Version 7.53a; Bruker Analytical X-ray Systems: Madison, WI.
- (16) Sheldrick, G. M. *Acta Crystallogr., Sect. A: Found. Crystallogr.* **2008**, *64*, 112–122.
- (17) Trofimenko, S.; Long, J. R.; Nappier, T.; Shore, S. G. In *Inorganic Syntheses*; Parry, W., Ed.; McGraw-Hill, Inc.: New York, 1970; Vol. 12, p 99.
- (18) Jones, H. O.; Tasker, H. S. *J. Chem. Soc., Trans.* **1909**, *95*, 1904–1909.
- (19) Bjerrum, J.; McReynolds, J. P. In *Inorganic Syntheses*; Fernelius, W. C., Ed.; McGraw-Hill, Inc.: New York, 1946; Vol. 2, p 216.
- (20) Lewis, G. R.; Dance, I. *J. Chem. Soc., Dalton Trans.* **2000**, 3176–3185.
- (21) Novitchi, G.; Wernsdorfer, W.; Chibotaru, L. F.; Costes, J. P.; Anson, C. E.; Powell, A. K. *Angew. Chem., Int. Ed.* **2009**, *48*, 1614–1619.
- (22) (a) Ishikawa, N.; Sugita, M.; Wernsdorfer, W. *Angew. Chem., Int. Ed.* **2005**, *44*, 2931–2935. (b) Lin, P. H.; Burchell, T. J.; Clérac, R.; Murugesu, M. *Angew. Chem., Int. Ed.* **2008**, *47*, 8848–8851. (c) Luis, F.; Martínez-Pérez, M. J.; Montero, O.; Coronado, E.; Cardona-Serra, S.; Martí-Gastaldo, C.; Clemente-Juan, J. M.; Sesé, J.; Drung, D.; Schurig, T. *Phys. Rev. B* **2010**, *82*, 060403. (d) Habib, F.; Lin, P.-H.; Long, J.; Korobkov, I.; Wernsdorfer, W.; Murugesu, M. *J. Am. Chem. Soc.* **2011**, *133*, 8830–8833.